

# Carbon isotopic fractionation during a mesocosm bloom experiment dominated by *Emiliana huxleyi*: Effects of CO<sub>2</sub> concentration and primary production

Albert Benthien<sup>a,\*</sup>, Ingrid Zondervan<sup>a</sup>, Anja Engel<sup>a</sup>, Jens Hefter<sup>a</sup>,  
Anja Terbrüggen<sup>a</sup>, Ulf Riebesell<sup>b</sup>

<sup>a</sup> Alfred-Wegener-Institut für Polar- und Meeresforschung, Am Handelshafen 12, D-27570 Bremerhaven, Germany

<sup>b</sup> Leibniz-Institut für Meereswissenschaften (IFM-Geomar), Düsternbrooker Weg 20, 24105 Kiel, Germany

Received 19 December 2005; accepted in revised form 8 December 2006; available online 27 December 2006

## Abstract

We investigated the effect of CO<sub>2</sub> and primary production on the carbon isotopic fractionation of alkenones and particulate organic matter (POC) during a natural phytoplankton bloom dominated by the coccolithophore *Emiliana huxleyi*. In nine semi-closed mesocosms (~11 m<sup>3</sup> each), three different CO<sub>2</sub> partial pressures (*p*CO<sub>2</sub>) in triplicate represented glacial (~180 ppmv CO<sub>2</sub>), present (~380 ppmv CO<sub>2</sub>), and year 2100 (~710 ppmv CO<sub>2</sub>) CO<sub>2</sub> conditions. The largest shift in alkenone isotopic composition (4–5‰) occurred during the exponential growth phase, regardless of the CO<sub>2</sub> concentration in the respective treatment. Despite the difference of ~500 ppmv, the influence of *p*CO<sub>2</sub> on isotopic fractionation was marginal (1–2‰). During the stationary phase, *E. huxleyi* continued to produce alkenones, accumulating cellular concentrations almost four times higher than those of exponentially dividing cells. Our isotope data indicate that, while alkenone production was maintained, the interaction of carbon source and cellular uptake dynamics by *E. huxleyi* reached a steady state. During stationary phase, we further observed a remarkable increase in the difference between δ<sup>13</sup>C of bulk organic matter and of alkenones spanning 7–12‰. We suggest that this phenomenon is caused mainly by a combination of extracellular release of <sup>13</sup>C-enriched polysaccharides and subsequent particle aggregation induced by the production of transparent exopolymer particles (TEP).

© 2007 Elsevier Inc. All rights reserved.

## 1. INTRODUCTION

The cosmopolitan coccolithophore *Emiliana huxleyi* is an important primary producer in the world's oceans (Westbroek et al., 1993; Tyrrell and Mercio, 2004). *E. huxleyi* is found in nearly all marine environments except the Arctic Ocean and high-latitude Southern Ocean. In terms of cell concentrations, it is frequently the dominant coccolithophore in waters cooler than 20 °C and warmer than 25 °C but coexists with a diversity of related species at intermediate temperatures (Winter et al., 1994; Brown

and Yoder, 1994). Blooms of *E. huxleyi* can cover wide areas of the ocean and have significant environmental impacts such as large calcium carbonate fluxes out of the surface waters and changes in the oceanic CO<sub>2</sub> uptake (e.g., Purdie and Finch, 1994; Robertson et al., 1994; Rost and Riebesell, 2004).

In addition to the spectacular blooms and their environmental effects, *E. huxleyi* is also known for synthesising a unique suite of biomarkers in form of long-chain alkenones (C<sub>37</sub>–C<sub>39</sub>). *E. huxleyi* is believed to be the predominant source of these biomarkers in the open ocean (Brassell, 1993), although the closely related species *Gephyrocapsa oceanica* may also be a significant source in warm water regions (Conte et al., 1995; Volkman et al., 1995). Alkenones are well preserved in marine sediments and their degree of

\* Corresponding author. Fax: +49 471 4831 2020.

E-mail address: [Albert.Benthien@awi.de](mailto:Albert.Benthien@awi.de) (A. Benthien).

unsaturation ( $U_{37}^{K'}$ ) and carbon isotopic composition ( $\delta^{13}C_{Alk}$ ) have been used to reconstruct palaeo-sea surface temperatures (e.g., Lyle et al., 1992; Rostek et al., 1993; Sachs and Lehman, 1999; Kienast et al., 2001) and ancient carbon dioxide concentrations (e.g., Jasper et al., 1994; Andersen et al., 1999; Pagani et al., 2005), respectively. While the applicability of alkenone unsaturation as a temperature proxy is widely accepted in palaeoceanographic research, it is still discussed controversially whether the carbon isotopic signal of alkenones can be used to reconstruct past- $CO_2$  concentrations (e.g., Riebesell et al., 2000; Benthien et al., 2002, 2005; Pagani et al., 2002, 2005; Schulte et al., 2004). Originally, this approach relied on the assumption that marine phytoplankton assimilates  $CO_2$  by passive diffusion. Consequently, aqueous  $CO_2$  concentration ( $[CO_{2aq}]$ ) would be one major factor controlling the carbon isotopic discrimination associated with the carbon fluxes in and out of the algal cell (François et al., 1993; Goericke and Fry, 1994). However, the results of subsequent laboratory and field experiments as well as theoretical considerations showed that photosynthetic carbon isotopic fractionation can be influenced by a number of physiological processes and environmental factors other than  $[CO_{2aq}]$ . These factors include carbon acquisition mechanisms, nutrient availability, irradiance, algal growth rate, and species-specific differences like cell size and geometry (e.g., Rau et al., 1996; Bidigare et al., 1997; Popp et al., 1998b; Keller and Morel, 1999; Riebesell et al., 2000; Rost et al., 2002). Focussing on taxon-specific biomarkers such as  $C_{37}$  alkenones provides a way to reduce the number of factors affecting the  $\delta^{13}C$  signal (Jasper and Hayes, 1990; Popp et al., 1998b). Next to its limited variation in cell size and geometry, *E. huxleyi* has probably not developed an efficient  $CO_2$ -concentrating mechanism and is thus more sensitive to  $CO_2$  variability compared to other phytoplankton species (Raven and Johnston, 1991; Badger et al., 1998; Rost et al., 2002). The results of recent sediment studies indicated that the alkenone  $\delta^{13}C$  record is primarily controlled by changes in algal growth rate due to the availability of nutrients rather than by  $[CO_{2aq}]$  (Benthien et al., 2002, 2005; Pagani et al., 2002; Schulte et al., 2004). Despite these limitations, Pagani et al. (2002, 2005) illustrated that the use of alkenone  $\delta^{13}C$  is a robust approach in the reconstruction of palaeo- $pCO_2$  levels if nutrient concentrations can be reasonably estimated.

Nevertheless, laboratory experiments and sediment studies also emphasised the fact that there are still some issues that need to be resolved before the isotopic signal of alkenones can be used reliably as a palaeoceanographic proxy (for a review see Laws et al., 2001). Of particular concern is the time of production and metabolic role of alkenones in the cell and how varying environmental conditions, notably  $[CO_{2aq}]$ , affect isotopic fractionation over the entire course of a natural bloom of alkenone-producing algae. Since laboratory studies cannot completely recreate the sum of environmental conditions and physiological factors which may influence the isotopic signal in the ocean we designed an experimental, semi-closed setup that allows the modification of  $[CO_{2aq}]$  in large seawater enclosures while the remaining environmental conditions

could be maintained as natural as possible. Here, we investigated bulk and alkenone isotopic fractionation during the development and decline of a natural plankton bloom dominated by the coccolithophore *E. huxleyi* exposed to three different  $CO_2$  concentrations.

## 2. MATERIAL AND METHODS

### 2.1. Experimental set-up

The experiment was conducted between 31 May and 25 June 2001 at the Marine Biological Station of the University of Bergen, Norway (EU-Large Scale Facility). The station is located at Espeland in the Raunefjord (60.3°N, 5.2°E), 20 km south of Bergen. The following paragraphs give a brief overview of the experimental set-up. Complete details of the experiment, mesocosm design and operation can be found in Engel et al. (2005) and Williams and Egge (1998).

Nine transparent polyethylene bags (2 m in diameter, 4.25 m deep,  $\sim 11 m^3$ ) were located on the southern side of a small raft, moored approximately 200 m from the shore. The enclosures were filled with unfiltered, nutrient-poor (post-bloom) fjord water from 2 m water depth. After filling, each mesocosm was covered with a transparent gas-tight tent constructed of ETFE foil (Foiltec GmbH, Bremen, Germany) which allows for 95% light transmission of the complete sunlight spectrum.

Three different atmospheric and seawater  $pCO_2$  levels (700, 380, and 180 ppmv) were adjusted in triplicate. The levels corresponded to approximately 'year 2100' (700 ppmv, assuming the IPCC's 'business as usual' scenario IS92a; high- $pCO_2$  mesocosms, MC 1–3), 'present' (380 ppmv; present- $pCO_2$  mesocosms, MC 4–6), and 'glacial' atmospheric  $CO_2$  levels (180 ppmv; low- $pCO_2$ -mesocosms, MC 7–9). The adjustment was achieved by aerating the water and the tents with either  $CO_2$ -enriched, unaltered or  $CO_2$ -free air. After four days of  $CO_2$ -adjustment the desired  $pCO_2$  levels in the water were reached (June 6, hereafter referred to as day 0) and the bubbling of the water column was stopped in order to let the carbonate system evolve naturally in accordance with the development of a bloom. At the same time the aeration of the tents was continued to maintain the atmospheres above the water surface at 'year 2100', 'present', and 'glacial' conditions, respectively.

To promote the development of the coccolithophore bloom, nitrate and phosphate were added to each mesocosm on day 0 in a ratio of 30:1 yielding initial concentrations of about  $15.5 \mu mol l^{-1} NO_3$  and  $0.5 \mu mol l^{-1} PO_4$ . After nutrient addition, the water in the mesocosms was gently mixed by means of an airlift system (Egge and Aksnes, 1992) to keep particles in suspension. For this purpose the same air as for the aeration of the tents was used.

As of day 0, the experiment was monitored over a 21 day period. In the following, time is referred to as  $d_x$  with  $x$  as the number of days after nutrient addition. Temperature and salinity profiles (CTD model SD204, SAIV A/S) as well as water samples were taken on a daily basis between 9:00 and 11:00 h. Water samples were taken at the same time

by gentle vacuum pumping of 20 l volume from 0.5 m depth. After transfer to the on-shore laboratory, sub-samples for the different analyses were taken immediately.

## 2.2. Sampling and analysis

A complete overview of the sampling procedures and analyses of the entire experiment is given in Engel et al. (2005). In addition, the monitoring and measurement of the carbonate system is described in detail by Delille et al. (2005). Here, we briefly describe sampling and analyses of the parameters relevant for the present study.

Nitrate and nitrite were determined from GF/F-filtered and poisoned (0.1% HgCl<sub>2</sub>) samples with an auto-analyser (AA II) within 4 months at the home laboratory. Phosphate was measured on the day of sampling using the methods of Koroleff and Grasshof (1983). Total particulate carbon (TPC) and particulate organic carbon (POC) were determined by elemental analysis from 1.0 l (d<sub>0</sub>–d<sub>12</sub>) or 0.5 l (d<sub>13</sub>–d<sub>21</sub>) samples filtered through pre-combusted (500 °C, 24 h) glass fibre filters (GF/F Whatman) using gentle vacuum filtration (~200 mbar). Prior to the measurement, POC-filters were fumed 2 h with saturated HCl to remove all particulate inorganic carbon and dried for 2 h at ~50 °C. TPC, POC and δ<sup>13</sup>C values were subsequently measured on a Europa Scientific ANCA SL 20-20 mass spectrometer, with a precision of ±0.5 μg C and ±0.5‰, respectively. Particulate inorganic carbon (PIC) was calculated by subtracting POC from TPC. To determine isotopic composition of dissolved inorganic carbon (δ<sup>13</sup>C<sub>DIC</sub>), 8 ml of the culture medium was fixed with HgCl<sub>2</sub>. Extractions and measurements were performed in the laboratory of H.J. Spero, University of California, Davis (USA), with a precision of ±0.11‰. Isotopic compositions are always reported relative to the VPDB standard.

Seawater partial pressure of CO<sub>2</sub> (*p*CO<sub>2</sub>) was measured using an equilibrator coupled to an infra-red gas analyzer (Li-Cor® 6262). The system was calibrated daily to air standards containing CO<sub>2</sub> at nominal mixing ratios of 0, 350, and 800 (±0.5) ppmv. Water temperature at the inlet of the pump and in the equilibrator was measured simultaneously using Li-Cor® sensors (for details see Delille et al., 2005).

Cell counts of phytoplankton and bacteria were performed with a FACSCalibur flow-cytometer (Becton Dickinson®) equipped with an air-cooled laser providing 0.015 W at 488 nm and with standard filter set-up. The fresh samples were analysed at high flow rate (~70 μl min<sup>-1</sup>) with the addition of 1-μm fluorescent beads (Molecular Probes). Autotrophic groups were discriminated on the basis of their forward or right angle light scatter (FALS, RALS) and chlorophyll (and phycoerythrin for *Synechococcus* and cryptophyte populations) fluorescence (Engel et al., 2005).

The net-specific growth rate ( $\mu$ ) of *E. huxleyi* was estimated from changes in cell concentrations according to Eq. (1), where  $C_i$  and  $C_{i+1}$  represent the cell concentrations at two consecutive days, and  $\Delta t$  is the corresponding time in days:

$$\mu = \frac{\ln C_{i+1} - \ln C_i}{\Delta t} \quad (1)$$

For alkenone analysis one mesocosm (MC) for each *p*CO<sub>2</sub> level (MC 2, MC 4, and MC 7) was sampled. For this purpose, water samples of known volume (4–10 l) were filtered onto pre-combusted (500 °C, 8 h), 47 mm diameter glass fibre filters (Whatman GF/F) using gentle vacuum (~200 mbar). Each filter was wrapped in aluminium foil. On d<sub>24</sub>, the particulate matter which had accumulated at the bottom of the mesocosm bags was sampled by gentle vacuum pumping and subsequently transferred into a small vial. Not a sediment by classical definition, this material or extracts of it are hereafter referred to as ‘sedimentary accumulation’ or ‘accumulated’.

Filters and vials were immediately frozen (–20 °C) after sampling and stored frozen until analysis. In the home laboratory the filters were freeze dried and alkenones were extracted by using pressurized liquid extraction (ASE 200, Dionex Corp., USA; Schantz et al., 1997; Calvo et al., 2003) with dichloromethane/methanol (9/1, v/v), 120 °C, 1450 psi for 13 min. The extracts were desalted, dried with Na<sub>2</sub>SO<sub>4</sub> and concentrated over N<sub>2</sub>. In order to remove possibly interfering esters the samples were saponified by adding 0.5 ml 0.1 M KOH in methanol/water (9/1, v/v) and subsequent heating to 90 °C in a capped vial for 2 h.

Alkenone concentrations were determined using an Agilent 6890 gas chromatograph (GC) with flame ionization detection (FID). The GC was equipped with a J&W DB1-MS column (60 m × 320 μm × 0.25 μm) and a cooled injection system (CIS 4, Gerstel GmbH, Germany). The GC temperature was programmed as follows: 35–200 °C at 15 °C min<sup>-1</sup> (1 min initial time) and 200–320 °C at 2 °C min<sup>-1</sup> with a 20 min hold at 320 °C. All reported alkenone concentrations have been corrected for GC recovery of internal *n*-alkane standards (*n*-C<sub>36</sub>, *n*-C<sub>37</sub>, *n*-C<sub>38</sub>, *n*-C<sub>41</sub>) added to each sample prior to injection.

The alkenone unsaturation index U<sub>37</sub><sup>K'</sup> was calculated according to Eq. (2) where [C<sub>37:2</sub>] and [C<sub>37:3</sub>] are the concentrations of the di- and tri-unsaturated C<sub>37</sub>-alkenone, respectively (Prahl and Wakeham, 1987):

$$U_{37}^{K'} = \frac{[C_{37:2}]}{[C_{37:2}] + [C_{37:3}]} \quad (2)$$

Compound-specific carbon isotope analysis (irm-GC/MS) of C<sub>37</sub>-alkenones (δ<sup>13</sup>C<sub>37:X</sub>) was carried out on a HP 6890 GC coupled via a Finnigan GCC-II-interface to a Finnigan Delta<sup>plus</sup> XL mass spectrometer. Samples were injected in pulsed-splitless mode and compound separation was achieved on a J&W DB1-MS capillary column (length = 60 m, i.d. = 0.32 mm, film thickness = 0.25 μm, carrier gas = helium). The GC temperature was programmed from 30 °C (5 min isothermal) to 150 °C (15 °C/min), from 150 °C to 320 °C at 3 °C/min, and held at 320 °C for 25 min. Several CO<sub>2</sub>-pulses of known δ<sup>13</sup>C value were introduced to the mass spectrometer at the beginning of each run. The alkenone-fractions contained four internal *n*-alkane standards (C<sub>36</sub>–C<sub>38</sub>, C<sub>41</sub>) and their known carbon isotopic composition was used as a quality check during the course of the measurements. Carbon isotope ratios are

notated as  $\delta$ -values (‰) relative to the VPDB-standard and the  $\delta^{13}\text{C}$ -value of the  $n\text{-C}_{38}$  alkane eluting immediately before the  $\text{C}_{37}$ -alkenone cluster was used as reference. Reported  $\delta^{13}\text{C}$  values are calculated as averages of at least triplicate analyses. Instrumental precision, as monitored by the  $n\text{-C}_{37}$  and  $n\text{-C}_{41}$  alkanes resulted in standard deviations better than  $0.2\text{‰}$ .

### 2.3. Isotopic fractionation $\epsilon$

The carbon isotopic composition of dissolved molecular  $\text{CO}_2$  ( $\delta^{13}\text{C}_{\text{CO}_{2\text{aq}}}$ ) was calculated from  $\delta^{13}\text{C}_{\text{DIC}}$  following the equation provided by Rau et al. (1996) based on Mook et al. (1974):

$$\delta^{13}\text{C}_{\text{CO}_{2\text{aq}}} = \delta^{13}\text{C}_{\text{DIC}} + 23.644 - \frac{9701.5}{T_k} \quad (3)$$

where  $T_k$  is the absolute temperature in Kelvin.

The isotopic fractionation of POC ( $\epsilon_{\text{POC}}$ ) and  $\text{C}_{37}$ -alkenones ( $\epsilon_{\text{Alk}}$ ) relative to that of  $\text{CO}_{2\text{aq}}$  was calculated according to Freeman and Hayes (1992):

$$\epsilon_{\text{POC}} = \left( \frac{\delta^{13}\text{C}_{\text{CO}_{2\text{aq}}} + 1000}{\delta^{13}\text{C}_{\text{POC}} + 1000} - 1 \right) \times 1000 \quad (4)$$

$$\epsilon_{\text{Alk}} = \left( \frac{\delta^{13}\text{C}_{\text{CO}_{2\text{aq}}} + 1000}{\delta^{13}\text{C}_{37:\text{X}} + 1000} - 1 \right) \times 1000 \quad (5)$$

where  $\delta^{13}\text{C}_{\text{POC}}$  and  $\delta^{13}\text{C}_{37:\text{X}}$  are the isotopic compositions of POC and  $\text{C}_{37}$ -alkenones, respectively.

## 3. RESULTS

### 3.1. Physical environment

The day length during the study period increased from 20.3 h at the beginning of the experiment to 22.7 h on day 15 (summer solstice). The average photosynthetically active radiation (PAR) during daytime was  $598 \pm 213 \mu\text{mol photons m}^{-2} \text{s}^{-1}$  and ranged from 127 to  $836 \mu\text{mol}$

$\text{photons m}^{-2} \text{s}^{-1}$  (the light sensor was located on the raft at  $\sim 2.5$  m above sea surface). Water temperature increased more or less steadily over the course of the experiment from  $\sim 10$  to  $\sim 13$  °C. Daily CTD casts showed virtually no variation of salinity with depth and only minor temperature variation ( $< 0.2$  °C) indicating homogeneous vertical mixing of the non-particulate parameters in the mesocosms (Engel et al., 2005).

### 3.2. $p\text{CO}_2$ and bloom development

At the beginning of the experiment ( $d_0$ ),  $p\text{CO}_2$  levels were adjusted to  $713 \pm 6.0$  ppmv in the high- $\text{CO}_2$  scenario (MC 1–3), to  $414 \pm 11$  ppmv in the mesocosms with ‘present’ conditions (MC 4–6), and to  $190 \pm 2.4$  ppmv in the low- $\text{CO}_2$  mesocosms (MC 7–9). Due to the development of the bloom,  $\text{CO}_2$  concentrations in the water decreased strongly until  $d_{15}$  and remained constant or increased slightly until  $d_{21}$ . As shown in Fig. 1, the magnitude of  $p\text{CO}_2$  change in the high- $\text{CO}_2$  scenario is  $\sim 6$  times higher than in the low- $\text{CO}_2$  mesocosms. This phenomenon can be explained by the lower buffering capacity of the carbonate system at lower pH values (Delille et al., 2005).

In contrast to the  $\text{CO}_2$  levels, nutrient concentrations decreased uniformly in the three mesocosms from  $15 \mu\text{mol l}^{-1}$  (nitrate) and  $0.5 \mu\text{mol l}^{-1}$  (phosphate) at  $d_0$  to values below the detection limit between  $d_{12}$  and  $d_{14}$  (Figs. 2a and b). Net growth of the phytoplankton community was detectable after  $d_5$  in all of the mesocosms and induced an increase in Chlorophyll *a* (Chl *a*) concentration from about  $1 \mu\text{g l}^{-1}$  pre-bloom concentration to values between 6.5 and  $12.5 \mu\text{g l}^{-1}$  at the peak of the bloom on  $d_{14}$ . The *E. huxleyi* pre-bloom phase was characterized by a dominance of both *Synechococcus* spp. and autotrophic flagellates (mainly *Micromonas* spp.) which reached maximum cell abundances between  $d_5$  and  $d_7$ , respectively (data not shown; see Engel et al., 2005). Subsequently, cell numbers decreased sharply and remained low until the end of the experiment ( $< 10^6$  cells  $\text{l}^{-1}$ ).

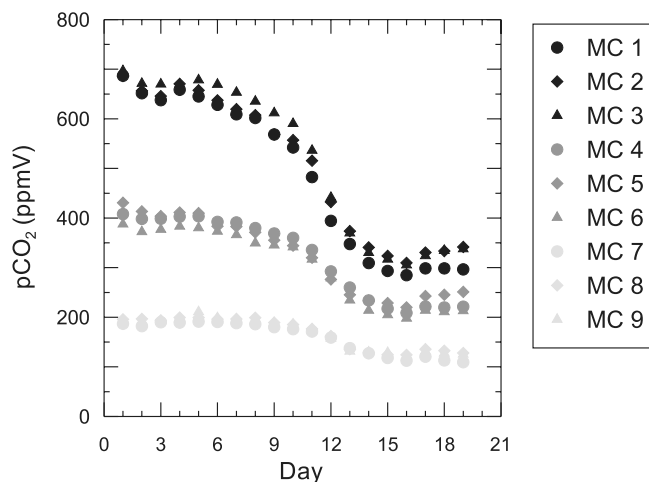


Fig. 1. The development of  $p\text{CO}_2$  during the experiment.

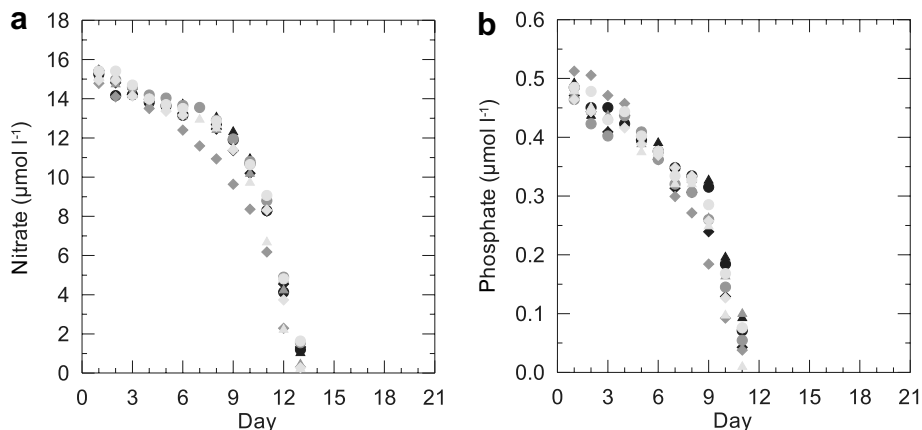


Fig. 2. The decrease of inorganic nutrients (a) nitrate and (b) phosphate. Symbols as in Fig. 1.

### 3.3. *E. huxleyi* cell numbers and POC

The initial cell abundances ( $d_3$ ) of *E. huxleyi* were between  $0.05 \times 10^6$  cells  $l^{-1}$  (MC 7) and  $0.19 \times 10^6$  cells  $l^{-1}$  (MC 5). Until  $d_5$  cell numbers remained below  $0.4 \times 10^6$  cells  $l^{-1}$ . As of  $d_6$  cell numbers increased exponentially at a rate between 0.37 and  $0.54 d^{-1}$  until growth was limited by nutrient depletion ( $d_{14}$ – $d_{15}$ ). Maximum cell abundances were reached between  $d_{14}$  and  $d_{20}$  and varied between  $22 \times 10^6$  cells  $l^{-1}$  (MC 8) and  $62 \times 10^6$  cells  $l^{-1}$  (MC 4) (Fig. 3). An exception to this was MC 1 where *E. huxleyi* cell numbers continued to increase until the end of the experiment. Despite a large variability among all mesocosms, Engel et al. (2005) demonstrated that until  $d_{14}$  the average net-specific growth rates in the low- $pCO_2$  treatments were significantly higher ( $0.50 \pm 0.26 d^{-1}$ ;  $n = 36$ ) than in the high- $pCO_2$  treatment ( $0.43 \pm 0.19 d^{-1}$ ;  $n = 36$ )

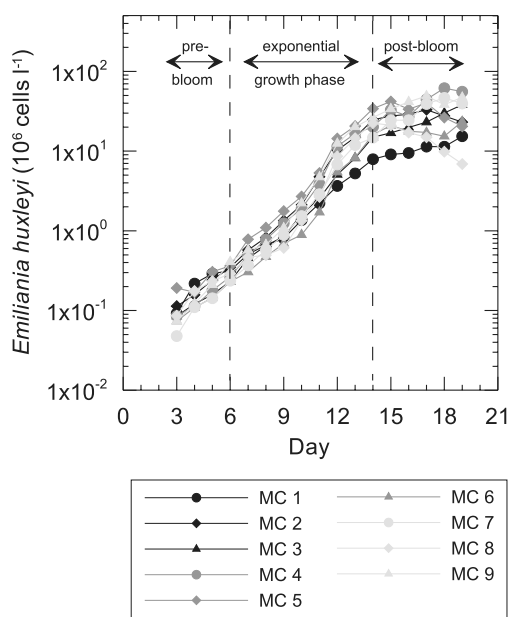


Fig. 3. *Emiliana huxleyi* cell numbers over time.

and slightly higher than in the present- $pCO_2$  scenario ( $0.47 \pm 0.26 d^{-1}$ ;  $n = 36$ ). Presumably, these differences were caused by variations in particle sinking rather than by varying cell division rates (Engel et al., 2005; Delille et al., 2005).

As of  $d_6$ , *E. huxleyi* cell growth induced a rapid increase in POC concentration ([POC]) (Table 1). Starting with an average concentration of  $17 \mu mol l^{-1}$ , [POC] went up more or less uniformly in all mesocosms until the onset of nutrient depletion (Fig. 4). Thereafter, the increase became highly variable with maximum values per mesocosm between  $76 \mu mol l^{-1}$  (MC 1;  $d_{16}$ ) and  $219 \mu mol l^{-1}$  (MC 4;  $d_{19}$ ). In this context, it is important to note that the particle concentration during the course of the bloom was most likely affected by differences in the initial distribution of cells and zooplankton, as well as by particle sinking and grazing (Engel et al., 2005).

The average carbon isotopic composition of POC ( $\delta^{13}C_{POC}$ ) at the beginning of the experiment was  $-23.7 \pm 0.8\text{‰}$  in the high- $pCO_2$  treatment,  $-23.1 \pm 0.2\text{‰}$  in the present- $pCO_2$  treatment, and  $-22.3 \pm 0.1\text{‰}$  in the low- $pCO_2$  treatment (Fig. 5). The different values can be explained by the different  $\delta^{13}C$  values of  $CO_{2aq}$  at  $d_0$  which were  $-12.7 \pm 0.5\text{‰}$ ,  $-11.9 \pm 0.3\text{‰}$ , and  $-11.0 \pm 0.2\text{‰}$  for the high-, present-, and low- $pCO_2$  treatment, respectively (Fig. 6). This is also demonstrated in Fig. 7 which shows that there is no treatment-related difference in the carbon isotopic fractionation of POC ( $\epsilon_{POC}$ ) at the beginning of the experiment. With the onset of the bloom, however, isotopic fractionation and hence  $\delta^{13}C_{POC}$  developed quite differently. In the high- and present- $pCO_2$  treatment,  $\delta^{13}C_{POC}$  first decreased by 2–3‰ to values between  $-26.2\text{‰}$  and  $-23.9\text{‰}$ . Thereafter,  $\delta^{13}C_{POC}$  increased rapidly and eventually reached maximum values between  $-21.3\text{‰}$  and  $-16.5\text{‰}$  in the high- $pCO_2$  treatment and  $-16.3\text{‰}$  and  $-10.0\text{‰}$  in the present- $pCO_2$  scenario ( $d_{17}$ – $d_{19}$ ). With the exception of MC 7, we found no initial  $\delta^{13}C_{POC}$  drop in the low- $pCO_2$  treatment. Here, the isotopic composition of POC increased constantly to maximum values similar to those of the present- $pCO_2$  scenario ( $-16.1$  to  $-9.5\text{‰}$ ). At the end of the experiment the observed isotope values in all mesocosms covered a range

Table 1

Regression analysis for the relationships between different parameters determined during the bloom experiment ( $y = ax + b$ )

	$p\text{CO}_2$ treatment	Days	$a$	$\pm\text{SD}$	$b$	$\pm\text{SD}$	$r^2$	$n$
$\epsilon_{\text{POC}} : [\text{POC}]$ (‰ : $\mu\text{M}$ )	High	6–14	-0.010	0.006	13.0	0.3	0.10	27
	Present	6–14	-0.048	0.006	13.6	0.3	0.74	27
	Low	6–14	-0.042	0.005	11.1	0.3	0.71	27
$\epsilon_{\text{POC}} : [\text{POC}]$ (‰ : $\mu\text{M}$ )	High	14–19	-0.080	0.013	16.8	1.3	0.75	15
	Present	14–19	-0.076	0.010	15.0	1.3	0.81	15
	Low	14–19	-0.060	0.008	12.2	1.1	0.80	15
$\epsilon_{\text{POC}} : [\text{POC}]$ (‰ : $\mu\text{M}$ )	High	6–19	-0.053	0.005	14.3	0.4	0.72	39
	Present	6–19	-0.069	0.004	14.2	0.3	0.91	39
	Low	6–19	-0.055	0.003	11.5	0.3	0.90	39
$\epsilon_{\text{Alk}} : [\text{Alkenones}]$ (‰ : $\mu\text{g/l}$ )	High	9–14	-0.082	0.006	16.0	0.1	0.96	8
	Present	9–14	-0.094	0.017	15.3	0.5	0.83	8
	Low	9–14	-0.147	0.007	14.3	0.1	0.99	8
$\epsilon_{\text{Alk}} : [\text{Alkenones}]$ (‰ : $\mu\text{g/l}$ )	High	14–19	-0.008	0.003	12.8	0.3	0.53	8
	Present	14–19	0.004	0.001	10.7	0.1	0.83	8
	Low	14–19	0.005	0.001	9.8	0.1	0.79	8
[POC] : [cell] ( $\mu\text{M} : \text{ml}^{-1}$ )	High	6–19	0.004	0.0002	24.9	3.2	0.87	39
	Present	6–19	0.003	0.0002	21.8	3.4	0.92	39
	Low	6–19	0.004	0.0001	23.5	2.4	0.96	39
[POC] : [cell] ( $\mu\text{M} : \text{ml}^{-1}$ )	High	14–19	0.002	0.0005	53.3	10.2	0.67	15
	Present	14–19	0.002	0.0004	54.9	14.2	0.71	15
	Low	14–19	0.003	0.0002	48.0	5.8	0.95	15

$n$  = number of samples;  $r^2$  = correlation coefficient squared; SD = standard deviation. The confidence intervals for the regression coefficients have been determined for 95% significance. No samples were taken on  $d_{18}$ .

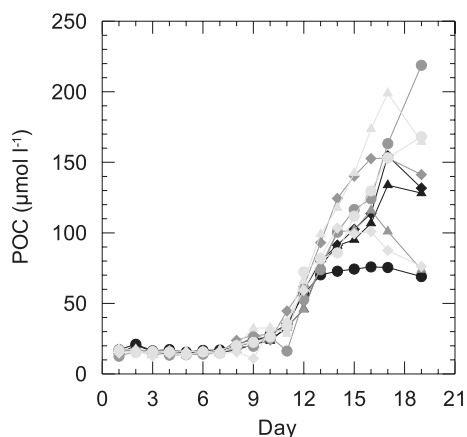


Fig. 4. The development of particulate organic carbon (POC). Lines and symbols as in Fig. 3.

of almost 12‰. Although no clear treatment-related effect could be observed during the post-bloom period, we found a relatively constant offset of 2–4‰ between the respective treatments over the course of the exponential growth phase (Fig. 5). As demonstrated by the isotopic fractionation values  $\epsilon_{\text{POC}}$  (Fig. 7), the treatment-related difference of  $\delta^{13}\text{C}_{\text{DIC}}$  and  $\delta^{13}\text{C}_{\text{CO}_{2\text{aq}}}$  can partly be accounted for this phenomenon (Fig. 6), but 1–2‰ of the offset remains unexplained. Generally, the decrease in  $\epsilon_{\text{POC}}$  correlated well with the increase in POC concentration. An exception to this was the high- $p\text{CO}_2$  treatment during the exponential growth phase. The results of the regression analyses are summarized in Table 1.

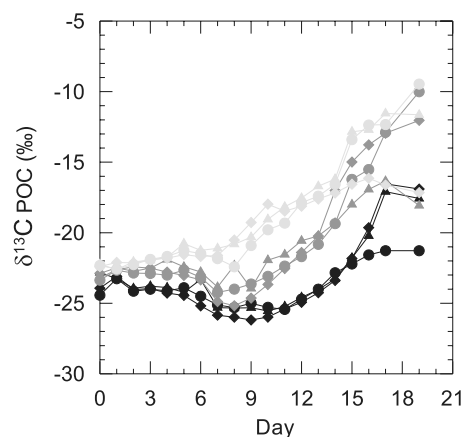


Fig. 5. The carbon isotopic composition of POC. Lines and symbols as in Fig. 3.

### 3.4. Alkenones

For alkenone analysis, one mesocosm was sampled from each treatment (MC 2, MC 4, and MC 7). Total alkenone concentrations were not reliably detectable until  $d_6$ . As of  $d_7$  they increased sharply from  $0.5 \mu\text{g l}^{-1}$  to maximum concentrations of  $105 \mu\text{g l}^{-1}$  ( $d_{17}$ ; MC 2),  $190 \mu\text{g l}^{-1}$  ( $d_{19}$ ; MC 4), and  $193 \mu\text{g l}^{-1}$  ( $d_{21}$ ; MC 7). Cellular alkenone concentrations, however, remained relatively constant during the exponential growth phase, at values between 0.8 and  $1.5 \text{ pg cell}^{-1}$  (Fig. 8). Upon nutrient depletion, cellular concentrations increased steadily by a factor of  $\sim 4$  to

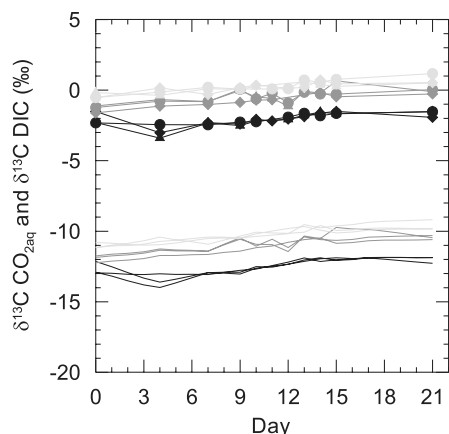


Fig. 6. The carbon isotopic composition of dissolved inorganic carbon (top, lines with symbols) and dissolved  $\text{CO}_2$  (bottom, lines). Lines and symbols as in Fig. 3.

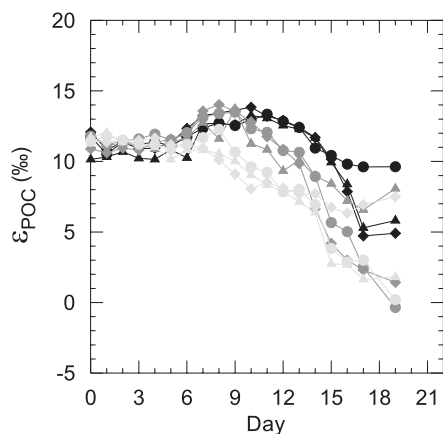


Fig. 7. The carbon isotopic fractionation of POC relative to  $\delta^{13}\text{C}_{\text{CO}_2(\text{aq})}$ . Lines and symbols as in Fig. 3.

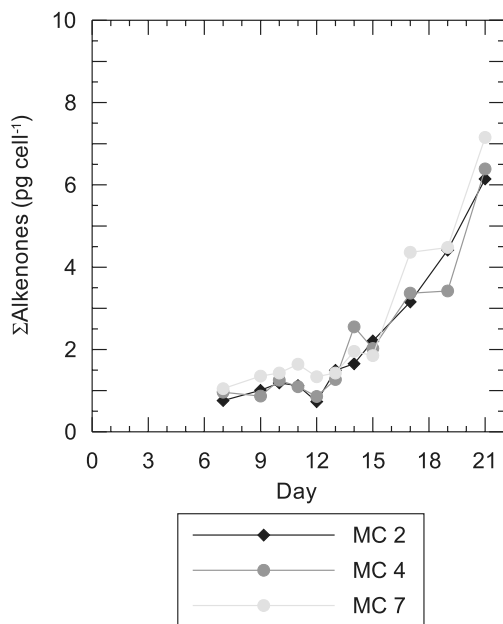


Fig. 8. The total  $\text{C}_{37-38}$  alkenone concentration per *E. huxleyi* cell.

maximum values between  $6.1 \text{ pg cell}^{-1}$  (MC 2) and  $7.2 \text{ pg cell}^{-1}$  (MC 7). Over the course of the bloom, the alkenone unsaturation index  $U_{37}^{K'}$  showed a very similar trend in all three mesocosms (Fig. 9). Initial  $U_{37}^{K'}$  values were between 0.26 and 0.29 and increased slightly to reach maximum values between 0.30 (MC 4) and 0.32 (MC 7) on  $d_{13}$ . Upon nutrient depletion,  $U_{37}^{K'}$  decreased again to 0.26 (MC 2)–0.28 (MC 7). Applying the established  $U_{37}^{K'}$ - $T$  calibration for *E. huxleyi* strain NEPCC 55a ( $U_{37}^{K'} = 0.034T + 0.039$ ; Prahl et al., 1988), these values translated into temperatures between 6.5 and  $8.3 \text{ }^\circ\text{C}$ . Compared to the daily measurements, alkenone  $U_{37}^{K'}$  thus underestimated the water temperature in the mesocosms by 3–4  $^\circ\text{C}$  at the beginning of the experiment to 5–6  $^\circ\text{C}$  on  $d_{19}$  (Fig. 9). Overall, the decrease in mean alkenone unsaturation with increasing mesocosm temperature correlated weakly ( $r^2 = 0.39$ ;  $n = 11$ ). The average  $U_{37}^{K'}$  of the ‘accumulated’ material in all three mesocosm was  $0.29 \pm 0.01$  which translates into  $7.5 \pm 0.2 \text{ }^\circ\text{C}$ . The average water temperature in the three mesocosm was  $11.8 \pm 1.1 \text{ }^\circ\text{C}$  over the course of the experiment yielding a difference of 4.8  $^\circ\text{C}$  between estimated and measured temperature.

Reliable results of the carbon isotopic composition of alkenones were obtained as of  $d_9$  (Fig. 10). With a  $\sim 2\text{‰}$  offset between the respective treatments, the  $\delta^{13}\text{C}$  of both the di- and tri-unsaturated  $\text{C}_{37}$ -alkenones increased constantly until  $d_{14}$  (MC 4, MC 7) and  $d_{15}$  (MC 2). With the onset of nutrient depletion,  $\delta^{13}\text{C}_{37:\text{X}}$  remained more or less constant at values of  $-23.7 \pm 0.1\text{‰}$  (MC 2),  $-21.4 \pm 0.2\text{‰}$  (MC 4), and  $-19.5 \pm 0.3\text{‰}$  (MC 7). Nearly identical values were measured for the ‘accumulated’ alkenones at the bottom of the three mesocosm bags. The alkenone carbon isotopic fractionation  $\varepsilon_{\text{Alk}}$  (Fig. 11) demonstrated that the main part of the observed isotopic offset between the treatments could be explained by the isotopic difference of  $\delta^{13}\text{C}_{\text{CO}_2(\text{aq})}$  or  $\delta^{13}\text{C}_{\text{DIC}}$ , respectively (Fig. 6). During the

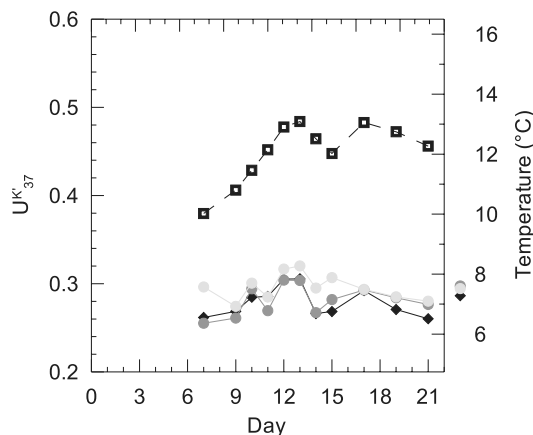


Fig. 9. Values of the alkenone unsaturation index  $U_{37}^{K'}$  (solid lines, closed symbols) for MC 2, MC 4, and MC 7. The average water temperature of the nine mesocosms is indicated by the dashed line (with open symbols). The  $U_{37}^{K'}$  values on the left y-axis correspond to the temperature scale on the right y-axis estimated after Prahl et al. (1988). The symbols outside the graph next to the right y-axis represent the ‘sedimentary accumulation’ values. Lines and symbols as in Fig. 8.

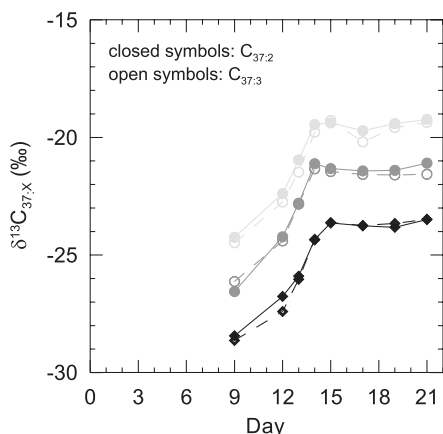


Fig. 10. The carbon isotopic composition of  $C_{37:2}$  (solid lines) and  $C_{37:3}$  (dashed lines) alkenones. The symbols outside the graph next to the right y-axis represent the 'sedimentary accumulation' values. Symbols as in Fig. 8.

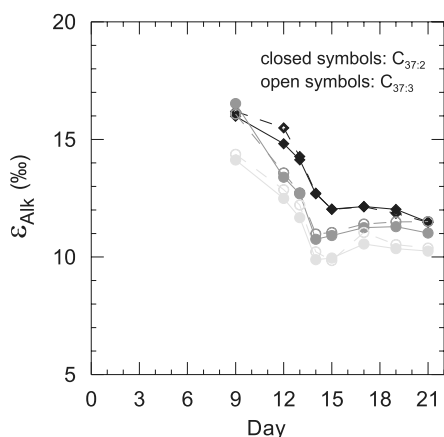


Fig. 11. The carbon isotopic fractionation of  $C_{37:2}$  and  $C_{37:3}$  alkenones relative to  $\delta^{13}C_{CO_2(aq)}$ . Lines and symbols as in Fig. 8.

exponential growth phase, the decrease in  $\epsilon_{Alk}$  correlated well with an increase in total alkenone concentration. The results of the regression analysis are shown in Table 1.

## 4. DISCUSSION

### 4.1. Alkenone unsaturation index $U_{37}^{K'}$

While the most often used  $U_{37}^{K'}$  calibration using *E. huxleyi* derived by Prah1 et al. (1988) has been validated globally by a nearly identical correlation between  $U_{37}^{K'}$  measurements in core-top sediments and annual mean temperatures of overlying surface waters (Müller et al., 1998), several other calibration studies based on laboratory cultures and water column particulates have reported significant deviations from this relationship (for an overview see Prah1 et al., 2000; Herbert, 2001). Like in our experiment, nearly all of these studies found lower  $U_{37}^{K'}$  values for a given growth temperature than one would have predicted from the Prah1/Müller regressions. Physiological factors such as nutrient availability (e.g., Epstein et al., 1998; Prah1 et al.,

2005) as well as genetic differences (e.g., Conte et al., 1998; Popp et al., 2006) have been suggested in order to explain this phenomenon. In a recent culture experiment at constant temperature (15 °C), Prah1 et al. (2003) found a decline of  $U_{37}^{K'}$  values by 0.11 units following growth limitation by nutrient depletion. This decrease in  $U_{37}^{K'}$  was accompanied by an increase in cellular alkenone concentration from 1.5–2 to 6  $\mu\text{g cell}^{-1}$  which is nearly identical to the values observed in the present study (Fig. 8). If we assume that nutrient depletion affected alkenone unsaturation in the mesocosm in a similar way, this may explain (1) the increasing offset between  $U_{37}^{K'}$  predicted and actually measured temperatures over the course of the experiment, and (2) the overall moderate  $U_{37}^{K'}$ -temperature correlation. This is further corroborated by the fact that until  $d_{13}$ , average  $U_{37}^{K'}$  responded much better to changes in water temperature ( $r^2 = 0.77$ ;  $n = 6$ ) than upon nutrient depletion ( $r^2 = 0.20$ ;  $n = 5$ ).

### 4.2. Isotopic fractionation in marine phytoplankton

Phytoplankton carbon isotope fractionation ( $\epsilon_p$ ) has been subject to substantial research over the last decade. Although a number of physiological and environmental factors have been identified to influence  $\epsilon_p$ , their relative importance for the overall isotopic signal is still uncertain. In principle, the magnitude of isotopic fractionation by marine phytoplankton is a function of the isotope effects associated with (1) the flux of inorganic carbon in and out of the cell, (2) the source of inorganic carbon and (3) the enzymatic carbon fixation (e.g., Hayes, 2001). Following the results of laboratory and field studies several models of photosynthetic  $^{13}C$  fractionation have been developed to describe the overall effect on the carbon isotopic composition of phytoplankton organic matter. While earlier models were restricted to only one carbon source (e.g., Sharkey and Berry, 1985; François et al., 1993; Laws et al., 1995; Rau et al., 1996), more recent considerations allow for uptake of bicarbonate ( $\text{HCO}_3^-$ ) and/or  $\text{CO}_2$  (e.g., Burkhardt et al., 1999; Keller and Morel, 1999). Burkhardt et al. (1999) extended a model from Sharkey and Berry (1985) in which isotope fractionation is ultimately determined by the isotopic composition of the carbon source and the leakage defined as the ratio of carbon efflux ( $F_{out}$ ) to carbon influx ( $F_{in}$ ):

$$\epsilon_p = a \times \epsilon_{b/d} + \epsilon_f \times \frac{F_{out}}{F_{in}} \quad (6)$$

where  $\epsilon_{b/d}$  represents the equilibrium discrimination between the carbon sources dissolved  $\text{CO}_2$  and  $\text{HCO}_3^-$  (ca.  $-10\text{‰}$ ; Mook et al., 1974) and  $a$  is the fractional contribution of  $\text{HCO}_3^-$  to total carbon uptake. The net isotope effect associated with the fixation of inorganic carbon is denoted by  $\epsilon_f$ . For  $C_3$  plants this includes not only the RubisCO-catalyzed  $\text{CO}_2$  fixation but also that of bicarbonate by PEP carboxylase. The latter process has a much smaller isotope effect and utilizes a carbon source that is enriched in  $^{13}C$  relative to dissolved  $\text{CO}_2$  (Hayes, 2001). For unicellular, eukaryotic phytoplankton,  $\epsilon_f$  was found to be in the range of 25–28‰ (Goericke et al., 1994; Popp et al., 1998b).

If there is no change in the inorganic carbon source (i.e., constant  $a$ ), Eq. (6) demonstrates that  $\epsilon_p$  decreases with decreasing leakage. An increasing portion of  $\text{HCO}_3^-$  uptake decreases the apparent isotope fractionation  $\epsilon_p$ , which is defined relative to the isotopic composition of  $\text{CO}_{2\text{aq}}$  (cf. Eqs. (4) and (5)). In the case of  $\text{CO}_{2\text{aq}}$  as the only carbon source and leakage being high ( $F_{\text{out}}/F_{\text{in}}$  approaching 1)  $\epsilon_p$  approaches  $\epsilon_f$ . At low leakage most of the carbon entering the cell is fixed and consequently  $\epsilon_p$  approaches the isotopic composition of the inorganic carbon source. In the case that  $\epsilon_p$  is lower than 0‰,  $\text{CO}_{2\text{aq}}$  can be excluded as being the only carbon source. On the other hand, only  $\epsilon_p$  values higher than 15–18‰ eliminate  $\text{HCO}_3^-$  as the sole carbon substrate.

The role of bicarbonate utilization and active carbon uptake by *E. huxleyi* has been discussed controversially in various studies. Based on the observation that *E. huxleyi* has comparatively low affinities for inorganic carbon, it has been hypothesized that this species may rely exclusively on diffusive  $\text{CO}_2$  supply for photosynthesis (Raven and Johnston, 1991; Badger et al., 1998). Recent studies, however, provide clear evidence that *E. huxleyi* has developed an inefficient albeit regulated  $\text{CO}_2$ -concentrating mechanism (CCM) and is able to use  $\text{HCO}_3^-$  as an inorganic carbon source for photosynthesis (e.g., Rost et al., 2002; Rost et al., 2003).

#### 4.3. Isotopic fractionation in *E. huxleyi* and POC

As already described in the result section, the experiment can be divided into three stages, namely the pre-bloom phase, the exponential phase, and the stationary phase (cf. Fig. 3). In the following, we will focus on carbon isotopic fractionation during the latter two phases which will be discussed successively. Regarding the isotopic composition of POC it has to be taken into account that due to the design of the experiment, *E. huxleyi* was certainly not the only source to the particulate organic carbon pool. We will therefore discuss isotopic fractionation of *E. huxleyi* based on changes in the  $\delta^{13}\text{C}$  of alkenones. An exception will be made for the early stage of the *E. huxleyi* bloom ( $d_6$ – $d_9$ ) since for this time no alkenone data were available (Fig. 11). It is generally known that lipids are depleted in  $^{13}\text{C}$  relative to total biomass ( $\Delta\delta$ ). Published data on  $\Delta\delta$  of  $\text{C}_{37}$  alkenones in culture experiments vary between 3.1‰ and 5.9‰ (Schouten et al., 1998; Popp et al., 1998a; Riebesell et al., 2000; Van Dongen et al., 2002). No systematic changes in these offsets have been observed with changes in growth rates or varying  $\text{CO}_2$  concentrations.

The initial increase in isotopic fractionation of bulk POC (Fig. 7) observed in the high- and present- $p\text{CO}_2$  treatments was most likely caused by an increasing contribution of *E. huxleyi*-derived,  $^{13}\text{C}$ -depleted organic carbon to the POC pool. According to the model expressed in Eq. (6), high  $\epsilon_p$  values require either relatively high cell leakage or a low contribution of  $\text{HCO}_3^-$  to total carbon uptake. Considering the high- $\text{CO}_2$  availability in the two treatments at the beginning of the experiment, either scenario or a combination of the two are conceivable. The availability of  $\text{CO}_2$  could also explain why the initial increase in  $\epsilon_{\text{POC}}$  did not

occur in the low- $p\text{CO}_2$  treatment, except for a slight increase in MC 7. With the decrease of  $p\text{CO}_2$  during the course of the bloom (Fig. 1) leakage has probably been reduced or the relative proportion of  $\text{HCO}_3^-$  uptake increased. Both scenarios can explain the observed uniform decrease in isotopic fractionation of alkenones (as well as POC) until nutrient depletion (Figs. 7 and 11). In this context it should be noted that in a recent culture experiment with *E. huxleyi*, Rost et al. (2006) found exactly opposite results, namely increasing leakage with decreasing  $[\text{CO}_2]$ . This observation can only be explained by an active CCM which would create the highest gradient between intracellular and external  $\text{CO}_2$  under low ambient  $\text{CO}_2$  concentration. In the case of our mesocosm experiment, this indicates that here *E. huxleyi* relied mainly on diffusive  $\text{CO}_2$  uptake, or that increasing bicarbonate utilization was responsible for the observed changes in isotopic fractionation. Rost et al. (2003) demonstrated that in *E. huxleyi* a gradual increase of  $\text{HCO}_3^-$  uptake relative to total carbon uptake occurred with decreasing  $p\text{CO}_2$ . However, the variations of their calculated uptake ratios ( $\text{CO}_2 : \text{HCO}_3^-$ ) are too small to entirely explain the changes in isotopic fractionation observed during the exponential growth phase in our study (Fig. 11).

Another important factor which is able to significantly affect carbon isotopic fractionation in *E. huxleyi* is a change in irradiance (Rost et al., 2002; Trimborn et al., submitted). Reported light saturation levels of photosynthetic carbon fixation range from 80 to over 500  $\mu\text{mol m}^{-2} \text{s}^{-1}$  and appear to be positively correlated to temperature (e.g., Zondervan et al., 2002; Paasche, 2002; Zondervan, in press). According to this, light saturation levels at temperatures between 10 and 13 °C should range between 80 and 150  $\mu\text{mol photons m}^{-2} \text{s}^{-1}$ . During the exponential growth phase, average light intensities frequently measured inside all mesocosms were always above these values and most of the times exceeded 300  $\mu\text{mol m}^{-2} \text{s}^{-1}$  by far (see also Delille et al., 2005). Hence, it can be excluded that variations in irradiance caused the observed trend in isotopic fractionation of *E. huxleyi*.

With the onset of nutrient exhaustion, the uniform decrease of  $\epsilon_{\text{Alk}}$  stopped and alkenone isotopic values remained unchanged until the end of the experiment (Figs. 10 and 11). Within a biosynthetic reaction network, this indicates that the isotopic composition of precursor molecules remained constant as well (e.g., Hayes, 2001) which in turn implies that cellular carbon uptake of *E. huxleyi* ceased or at least reached a steady state. On the other hand, alkenone production continued resulting in an increase of the cellular alkenone concentration up to 7  $\text{pg cell}^{-1}$  (Fig. 8) which is equivalent to approx. 5.6  $\text{pg cell}^{-1}$  alkenone-C. Like other microalgae, *E. huxleyi* is known to build up its carbohydrate and lipid stores in the stationary phase (e.g., Shifrin and Chisholm, 1981; Dunstan et al., 1993; Brown et al., 1996). However, while in other phytoplankton species the amount of lipid-carbon averages 15–25%, *E. huxleyi* incorporates up to 40–60% of carbon into the lipid fraction (Fernández et al., 1994, 1996). In exponentially growing cells alkenones comprise between 2% and 20% of total cellular carbon (Prahl et al., 1988; Pond and Harris,

1996; Conte et al., 1998). Under nutrient stress, values up to 39% have been reported (Prahl et al., 2003). This is in very good agreement with the results of our experiment, assuming that cellular concentrations of total organic carbon in *E. huxleyi* range from 6 to 15 pg cell<sup>-1</sup> in exponentially growing cells (Riebesell et al., 2000; Zondervan et al., 2002; Prahl et al., 2003) and up to 22 pg cell<sup>-1</sup> under stationary phase conditions (Fernández et al., 1994; Van Bleijswijk et al., 1994; Riegman et al., 2000).

The isotopic composition of biomass carbon in an algal cell is given by Eq. (7) (Hayes, 2001):

$$\delta_{\text{Biomass}} = X_{\text{NA}}\delta_{\text{NA}} + X_{\text{Prot}}\delta_{\text{Prot}} + X_{\text{Sacc}}\delta_{\text{Sacc}} + X_{\text{Lip}}\delta_{\text{Lip}} \quad (7)$$

where the subscripts NA, Prot, Sacc, and Lip, respectively refer to the compound classes nucleic acids and related materials, proteins, mono- and polysaccharides, and lipids of all kinds. The  $X$  terms, which sum to 1.0, refer to mole fractions of carbon and the  $\delta$  terms refer to the average carbon isotopic compositions.

Although exact estimates of the respective  $\delta$  values are not available, Eq. (7) demonstrates that the cellular increase of isotopically depleted alkenones during the stationary phase will result in a decrease of  $\Delta\delta^{13}\text{C}_{\text{Cell-Alk}}$ , the isotopic difference between total biomass and alkenones. Since at this time of the experiment *E. huxleyi* is by far the dominant phytoplankton species (Engel et al., 2005), it is remarkable that at the same time the isotopic difference between alkenones and POC (cf. Figs. 5 and 10) increased significantly. Moreover, the increase in POC is well correlated to *E. huxleyi* cell abundances (Table 1). This phenomenon of isotopic decoupling can be explained if one presumes that a considerable fraction of the <sup>13</sup>C-enriched POC is not part of intact *E. huxleyi* cells. Assuming an organic carbon quota of 22 pg cell<sup>-1</sup>, *E. huxleyi*-bound organic carbon indeed accounted for only 32–49% of POC (MC 2, MC 4, and MC 7; d<sub>17</sub>–d<sub>19</sub>). Engel et al. (2004) demonstrated that a considerable fraction of the remaining POC (~30%) is the result of TEP-induced aggregation processes which transferred carbon from the dissolved into the particulate polysaccharide pool. TEP (transparent exopolymer particles) are mainly carbohydrates and hence relatively carbon rich with C:N ratios of ~26. They originate from dissolved precursors and are known to favour particle aggregation (Engel, 2000; Engel and Passow, 2001). Dissolved polysaccharides are well known to be generated by extracellular release and constitute an important component of the labile fraction of DOC (e.g., Benner et al., 1992; Kepkay et al., 1993; Myklestad, 1995). Polysaccharides are furthermore noted to be enriched in <sup>13</sup>C compared to bulk organic carbon (e.g., Deines, 1980; Wong et al., 1975; Hayes, 2001). It has been shown that *E. huxleyi* cells produce and excrete an acidic polysaccharide which is assumed to be involved in the morphogenesis of coccoliths (De Jong et al., 1976; Van Emburg et al., 1986; Nanninga et al., 1996). These so-called coccolith polysaccharides (CP) contain a number of monosaccharides such as glucose, mannose, arabinose, and xylose (Fichtinger-Schepman et al., 1979). Van Dongen et al. (2002) have demonstrated that these monosaccharides were enriched in <sup>13</sup>C by 6‰ compared to bulk organic biomass and by 11‰ relative to alkenones. Together, the

above considerations indicate that the combination of extracellular release and the subsequent TEP-induced aggregation of <sup>13</sup>C-enriched polysaccharides caused the increase in particulate matter and in turn the observed isotopic decoupling of POC and alkenones. However, while we observed a generally good correlation between the increase in *E. huxleyi* cell abundances and POC concentration (Table 1) it should be taken into account that a certain amount of organic matter production is not directly linked to the *E. huxleyi* bloom. Apart from determining bacterial abundances (Rochelle-Newall et al., 2004) the heterotrophic food web has not been examined during this experiment. It thus remains elusive to what extent bacterial production and grazing contributed to the overall carbon isotopic budget. Moreover, it is conceivable that DOC fractions other than polysaccharides contributed to the aggregation processes such as it has been observed in a study by Kerner et al. (2003) analysing Elbe river water. Here, the authors also observed microparticles significantly enriched in <sup>13</sup>C compared to the DOC from which they originated. Whether this phenomenon has the potential to significantly affect the carbon isotopic composition of POC needs to be examined in more detailed studies with the focus on abiotic aggregation.

#### 4.4. Implications for the metabolic role of alkenones and their application as palaeoceanographic proxies

The use of alkenone unsaturation to estimate past sea-surface temperatures has gained wide acceptance (e.g., Müller et al., 1998; Prahl et al., 2000). While the findings from our mesocosm experiment do not question this approach they clearly demonstrate that (1) not all alkenone-producing algae display identical temperature responses for U<sub>37</sub><sup>K'</sup> and (2) the absolute value of sedimentary U<sub>37</sub><sup>K'</sup> may not be controlled exclusively by growth temperature at the sea surface. In accordance with the results of previous laboratory experiments (e.g., Conte et al., 1998; Epstein et al., 1998; Prahl et al., 2003), our data suggest that genetic differences and the physiological condition (i.e., nutrient limitation) of *E. huxleyi* cells could affect the U<sub>37</sub><sup>K'</sup> signal exported to the sediment. It is likely that part of the variability found in the global core-top calibration of U<sub>37</sub><sup>K'</sup> versus annual mean sea-surface temperature (Müller et al., 1998) could be accounted for by these effects.

In contrast to alkenone unsaturation, it is still discussed controversially whether the alkenone isotopic signal can be used to reconstruct palaeo-environmental conditions such as past-CO<sub>2</sub> concentrations or palaeo-nutrient levels (Riebesell et al., 2000; Benthien et al., 2002, 2005; Pagani et al., 2002, 2005; Rost et al., 2002; Schulte et al., 2004). In any case, there are still several issues that need to be resolved before alkenone isotopic fractionation can be applied confidently as a palaeoceanographic proxy.

A particular concern is defining the location and physiological function of alkenones in the cell. Since the degree of unsaturation varies as a function of growth temperature, it has been speculated that alkenones have a role in regulating membrane fluidity (e.g., Prahl and Wakeham, 1987; Brassell, 1993). More recently, it has been suggested that

*E. huxleyi* uses alkenones for metabolic storage (Bell and Pond, 1996; Epstein et al., 2001) or that their biosynthesis might be associated with the function of the coccolith-producing compartment (CPC) (Sawada and Shiraiwa, 2004). The hypothesis that alkenones serve as energy reserves has recently been corroborated by Eltgroth et al. (2005) who furthermore found evidence that alkenones as well as polyunsaturated long-chain alkenoates and alkenes (PULCA) are synthesised in the chloroplast and subsequently packaged into lipid bodies and exported to the cytoplasm. The results of our study support the idea of alkenones as metabolic storage molecules. Moreover, the isotopic pattern indicates that with the onset of nutrient depletion the cellular carbon uptake of *E. huxleyi* reached a steady state while alkenone production was continued. Whether this phenomenon is linked to the packaging and export of PULCA into cytoplasmic lipid bodies (Eltgroth et al., 2005) remains elusive.

The use of alkenone  $\delta^{13}\text{C}$  as a proxy for palaeo-environmental reconstructions relies on the premise that isotopic fractionation in *E. huxleyi* (and other alkenone-producing species) is largely determined by a small number of environmental and physiological conditions. The results of culture experiments and field studies (e.g., Bidigare et al., 1997; Riebesell et al., 2000; Laws et al., 2001; Rost et al., 2002) as well as sediment analyses (e.g., Benthien et al., 2002, 2005; Pagani et al., 2002; Schulte et al., 2004) consistently demonstrated that  $\epsilon_{\text{Alk}}$  is not primarily controlled by  $\text{CO}_2$  concentration but by algal growth rate and carbon uptake mechanisms. The latter are in turn influenced by variations in temperature, nutrient supply, and irradiance. In our mesocosm study, nutrient conditions as well as irradiance and temperature were more or less identical for each treatment. The results demonstrate that the influence of different  $\text{CO}_2$  concentrations on  $\epsilon_{\text{Alk}}$  is indeed marginal. Despite a difference in  $p\text{CO}_2$  of  $\sim 500$  ppmv, the isotopic fractionation varied by only 1–2‰ during the entire course of the experiment. Moreover, it is shown that the ‘accumulated’ signal found at the bottom of the mesocosm bags recorded this marginal difference in alkenone isotopic fractionation (Fig. 10). If these findings are representative for *E. huxleyi* in the natural environment, it would explain the low  $\text{CO}_2$ -sensitivity of  $\epsilon_{\text{Alk}}$  commonly observed in field and sediment studies. Our results further illustrate that the largest shift in alkenone isotopic composition (4–5‰) occurred during the exponential growth phase. The nutrient conditions at the beginning of the bloom were identical for each mesocosm and caused more or less similar growth rates during the exponential phase. It has to be speculated how different pre-bloom conditions (i.e., varying nutrient availability) or the timing of bloom termination (i.e., through viral infection) would have influenced the course of the bloom and consequently the isotopic fractionation of alkenones. Our results further demonstrated that the isotopic signal found in the ‘sedimentary accumulation’ reflected the late exponential or stationary growth phase. Hence, it is conceivable that varying nutrient conditions will easily mask the  $\text{CO}_2$ -related signal such as it has been observed in core-top sediments from various oceanographic regions (Benthien et al., 2002; Pagani et al., 2002). While the interpretation of alke-

none  $\delta^{13}\text{C}$  remains difficult, it is probably safe to say that it is not a suitable proxy for the reconstruction of palaeo- $\text{CO}_2$  concentration, especially when applied without knowledge of the respective bloom conditions. Further research is warranted to refine the understanding of alkenone biosynthesis and its physiological control to explore the environmental control on alkenone isotopic fractionation.

#### ACKNOWLEDGMENTS

We especially wish to thank the staff of the Marine Biological Station of the University of Bergen, in particular Clelia Booman, Jorun Egge, Erling Heggoy, and Jens Nejtgaard, who helped us conduct the experiment. Kai Buss and Michael Schlüter from the IUV at the University of Bremen assisted in the development of the experimental set-up. We are also grateful to Jean-Pierre Gattuso (Observatoire Océanologique de Villefranche sur Mer, France) who accomplished PAR measurements and Stéphane Jacquet (Station INRA d’Hydrobiologie Lacustre, France) for the phytoplankton cell counts. Bruno Delille, Gerald Langer, Gesine Mollenhauer, Uta Passow, Björn Rost, Silke Thoms, Sonja Schulte, and Kai Schulz provided fruitful discussions and helpful comments. Alex Sessions, Magnus Eek and two anonymous referees are acknowledged for their suggestions on improving the publication. This work was supported by the Alfred Wegener Institute for Polar and Marine Research and the European Commission Human Potential Programme HPRI-1999-0056.

#### REFERENCES

- Andersen N., Müller P. J., Kirst G., and Schneider R. R. (1999) Alkenone  $\delta^{13}\text{C}$  as a proxy for past  $\text{PCO}_2$  in surface waters: results from the Late Quaternary Angola Current. In *Use of Proxies in Paleooceanography: Examples from the South Atlantic*, (eds. G. Fischer and G. Wefer), pp. 469–488. Springer.
- Badger M. R., Andrews T. J., Whitney S. M., Ludwig M., Yellowlees D. C., Leggat W., and Price G. D. (1998) The diversity and coevolution of Rubisco, plastids, pyrenoids, and chloroplast-based  $\text{CO}_2$ -concentrating mechanisms in algae. *Can. J. Bot.* **76**, 1052–1071.
- Bell M. V., and Pond D. (1996) Lipid composition during growth of motile and coccolith forms of *Emiliania huxleyi*. *Phytochemistry* **41**, 465–471.
- Benner R., Pakulski J. D., McCarthy M., Hedges J. I., and Hatcher (1992) Bulk chemical characteristics of dissolved organic matter in the ocean. *Science* **255**, 1561–1564.
- Benthien A., Andersen N., Schulte S., Müller P. J., Schneider R. R., and Wefer G. (2002) Carbon isotopic composition of the  $\text{C}_{37:2}$  alkenone in core-top sediments of the South Atlantic Ocean: effects of  $\text{CO}_2$  and nutrient concentrations. *Global Biogeochem. Cycles* **16**. doi:10.1029/2001GB001433.
- Benthien A., Andersen N., Schulte S., Müller P. J., Schneider R. R., and Wefer G. (2005) The carbon isotopic record of the  $\text{C}_{37:2}$  alkenone in the South Atlantic: Last Glacial Maximum (LGM) vs. Holocene. *Palaeogeogr. Palaeoclimatol. Palaeoecol.* **221**, 123–140.
- Bidigare R. R., Fluegge A., Freeman K. H., Hanson K. L., Hayes J. M., Hollander D., Jasper J. P., King L. L., Laws E. A., Milder J., Millero F. J., Pancost R., Popp B. N., Steinberg P. A., and Wakeham S. G. (1997) Consistent fractionation of  $^{13}\text{C}$  in nature and in the laboratory: growth-rate effects in some haptophyte algae. *Global Biogeochem. Cycles* **11**, 279–292.
- Brassell S. C. (1993) Applications of biomarkers for delineating marine paleoclimatic fluctuations during the Pleistocene. In

- Org. Geochem.*, (eds. M.H. Engel and S.A. Macko), pp. 699–738. Plenum Press, New York.
- Brown C. W., and Yoder J. A. (1994) Coccolithophorid blooms in the global ocean. *J. Geophys. Res.* **99**, 7467–7482.
- Brown M. R., Dunstan G. A., Norwood S. J., and Miller K. A. (1996) Effects of harvest stage and light on the biochemical composition of the diatom *Thalassiosira pseudonana*. *J. Phycol.* **32**, 64–73.
- Burkhardt S., Riebesell U., and Zondervan I. (1999) Effects of growth rate, CO<sub>2</sub> concentration, and cell size on the stable carbon isotope fractionation in marine phytoplankton. *Geochim. Cosmochim. Acta* **63**, 3729–3741.
- Calvo E., Pelejero C., and Logan G. A. (2003) Pressurized liquid extraction of selected molecular biomarkers in deep sea sediments used as proxies in paleoceanography. *J. Chromatogr. A* **989**, 197–205.
- Conte M. H., Thompson A., Eglinton G., and Green J. C. (1995) Lipid biomarker diversity in the coccolithophorid *Emiliania huxleyi* (Prymnesiophyceae) and the related species *Gephyrocapsa oceanica*. *J. Phycol.* **31**, 272–282.
- Conte M. H., Thompson A., Lesley D., and Harris R. P. (1998) Genetic and physiological influences on the alkenone/alkenoate versus growth temperature relationship in *Emiliania huxleyi* and *Gephyrocapsa oceanica*. *Geochim. Cosmochim. Acta* **62**, 51–68.
- De Jong E. W., Bosch L., and Westbroek P. (1976) Isolation and characterization of a Ca<sup>2+</sup>-binding polysaccharide associated with coccoliths of *Emiliania huxleyi* (Lohmann) Kamptner. *Eur. J. Biochem.* **70**, 611–621.
- Deines P. (1980) The isotopic composition of reduced organic carbon. In *Handbook of environmental isotope geochemistry*, (eds. P. Fritz and J.C. Fontes), pp. 329–406. Elsevier.
- Delille B., Harlay J., Zondervan I., Jacquet S., Chou L., Wollast R. G. J., Bellerby R. G. J., Frankignoulle M., Borges A. V., Riebesell U., and Gattuso J.-P. (2005) Response of primary production and calcification to changes of pCO<sub>2</sub> during experimental blooms of the coccolithophorid *Emiliania huxleyi*. *Global Biogeochem. Cycles* **19**. doi:10.1029/2004GB002318.
- Dunstan G. A., Volkman J. K., Barrett S. M., and Garland C. D. (1993) Changes in the lipid composition and maximisation of the polyunsaturated fatty acid content of three microalgae grown in mass culture. *J. Appl. Phycol.* **5**, 71–83.
- Egge J. K., and Aksnes D. L. (1992) Silicate as regulating nutrient in phytoplankton competition. *Mar. Ecol. Prog. Ser.* **83**, 281–289.
- Eltgroth M. L., Watwood R. L., and Wolfe G. V. (2005) Production and cellular localization of neutral long-chain lipids in the haptophyte algae *Isochrysis galbana* and *Emiliania huxleyi*. *J. Phycol.* **41**, 1000–1009.
- Engel A. (2000) The role of transparent exopolymer particles (TEP) in the increase in apparent particle stickiness ( $\alpha$ ) during the decline of a diatom bloom. *J. Plankton Res.* **22**, 485–497.
- Engel A., and Passow U. (2001) Carbon and nitrogen content of transparent exopolymer particles (TEP) in relation to their Alcian Blue adsorption. *Mar. Ecol. Prog. Ser.* **219**, 1–10.
- Engel A., Thoms S., Riebesell U., Rochelle-Newall E., and Zondervan I. (2004) Polysaccharide aggregation as a potential sink of marine dissolved organic carbon. *Nature* **428**, 929–932.
- Engel A., Zondervan I., Aerts K., Beaufort L., Benthien A., Chou B., Delille B., Gattuso J.-P., Harlay J., Heemann C., Hoffmann S., Jacquet S., Nejstgaard J., Pizay M.-D., Rochelle-Newall E., Schneider U., Terbrüggen A., and Riebesell U. (2005) Testing the direct effect of CO<sub>2</sub> concentration on a bloom of the coccolithophorid *Emiliania huxleyi* in mesocosm experiments. *Limnol. Oceanogr.* **50**, 493–507.
- Epstein B. L., D'Hondt S., Quinn J. G., Zhang J., and Hargraves P. (1998) An effect of dissolved nutrient concentrations on alkenone-based temperature estimates. *Paleoceanography* **13**, 122–126.
- Epstein B. L., D'Hondt S., and Hargraves P. E. (2001) The possible metabolic role of C<sub>37</sub> alkenones in *Emiliania huxleyi*. *Org. Geochem.* **32**, 867–875.
- Fernández E., Balch W. M., Marañón E., and Holligan P. M. (1994) High rates of lipid biosynthesis in cultured, mesocosm and coastal populations of the coccolithophore *Emiliania huxleyi*. *Mar. Ecol. Prog. Ser.* **114**, 13–22.
- Fernández E., Marañón E., and Balch W. M. (1996) Intracellular carbon partitioning in the coccolithophorid *Emiliania huxleyi*. *J. Mar. Syst.* **9**, 57–66.
- Fichtinger-Schepman A. M. J., Kamerling J. P., Vliegenhart J. F. G., De Jong E. W., Bosch L., and Westbroek P. (1979) Composition of a methylated, acidic polysaccharide associated with coccoliths of *Emiliania huxleyi* (Lohmann) Kamptner. *Carbohydr. Res.* **69**, 181–189.
- François R., Altabet M. A., Goericke R., McCorkle D. C., Brunet C., and Poisson A. (1993) Changes in the  $\delta^{13}\text{C}$  of surface water particulate organic matter across the subtropical convergence in the SW Indian Ocean. *Global Biogeochem. Cycles* **7**, 627–644.
- Freeman K. H., and Hayes J. M. (1992) Fractionation of carbon isotopes by phytoplankton and estimates of ancient CO<sub>2</sub> levels. *Global Biogeochem. Cycles* **6**, 185–198.
- Goericke R., Montoya J. P., and Fry B. (1994) Physiology of isotopic fractionation in algae and cyanobacteria. In *Stable Isotopes in Ecology and Environmental Science*, (eds. K. Lajtha and R.H. Michener), pp. 187–221. Blackwell Science Publishers.
- Hayes J. M. (2001) Fractionation of carbon and hydrogen isotopes in biosynthetic processes. In *Stable Isotope Geochemistry*, (eds. J.W. Valley and D.R. Cole), vol. 43, pp. 225–277. Mineralogical Society of America.
- Herbert T. D., 2001. Review of alkenone calibrations (culture, water column, and sediments). *Geochem., Geophys., Geosyst.* **2**, Paper number 2000G000055.
- Jasper J. P., and Hayes J. M. (1990) A carbon isotope record of CO<sub>2</sub> levels during the late Quaternary. *Nature* **347**, 462–464.
- Jasper J. P., Hayes J. M., Mix A. C., and Prahl F. G. (1994) Photosynthetic fractionation of <sup>13</sup>C and concentrations of dissolved CO<sub>2</sub> in the central equatorial Pacific during the last 255,000 years. *Paleoceanography* **9**, 781–798.
- Keller K., and Morel F. M. M. (1999) A model of carbon isotopic fractionation and active carbon uptake in phytoplankton. *Mar. Ecol. Prog. Ser.* **182**, 295–298.
- Kepkay P. E., Niven S. E. H., and Milligan T. G. (1993) Low molecular weight and colloidal DOC production during a phytoplankton bloom. *Mar. Ecol. Prog. Ser.* **100**, 233–244.
- Kerner M., Hohenberg H., Ertl S., Reckermann M., and Spitz A. (2003) Self-organization of dissolved organic matter to micelle-like microparticles in river water. *Nature* **422**, 150–154.
- Kienast M., Steinke S., Stattegger K., and Calvert S. E. (2001) Synchronous tropical South China Sea SST change and Greenland warming during deglaciation. *Science* **291**, 2132–2134.
- Koroleff F., and Grasshof K. (1983) Determination of nutrients. In *Methods of Seawater Analyses*, (eds. K. Grasshof, M. Erhardt and K. Kremling), vol. 2, pp. 125–188. Verlag Chemie.
- Laws E. A., Popp B. N., Bidigare R. R., Kennicutt M. C., and Macko S. A. (1995) Dependence of phytoplankton carbon isotopic composition on growth rate and CO<sub>2aq</sub>: theoretical considerations and experimental results. *Geochim. Cosmochim. Acta* **59**, 1131–1138.
- Laws E. A., Popp B. N., Bidigare R. R., Riebesell U., Burkhardt S., and Wakeham S. G., 2001. Controls on the molecular distribution and carbon isotopic composition of alkenones in

- certain haptophyte algae. *Geochem., Geophys., Geosyst.* **2**, Paper number 2000GC000057.
- Lyle M. W., Prahl F. G., and Sparrow M. A. (1992) Upwelling and productivity changes inferred from a temperature record in the central equatorial Pacific. *Nature* **355**, 812–815.
- Mook W. G., Bommerson J. C., and Staverman W. H. (1974) Carbon isotope fractionation between dissolved bicarbonate and gaseous dioxide. *Earth Planet. Sci. Lett.* **22**, 169–176.
- Müller P. J., Kirst G., Ruhland G., von Storch I., and Rosell-Melé (1998) Calibration of the alkenone paleotemperature index  $U_{37}^K$  based on core-tops from the eastern South Atlantic and the global ocean (60°N–60°S). *Geochim. Cosmochim. Acta* **62**, 1757–1772.
- Myklestad S. M. (1995) Release of extracellular products by phytoplankton with special emphasis on polysaccharides. *The Science of the Total Environment* **165**, 155–164.
- Nanninga H. J., Ringenaldus P., and Westbroek P. (1996) Immunological quantitation of a polysaccharide formed by *Emiliana huxleyi*. *J. Mar. Syst.* **9**, 67–74.
- Paasche E. (2002) A review of the coccolithophorid *Emiliana huxleyi* (Prymnesiophyceae), with particular reference to growth, coccolith formation, and calcification-photosynthesis interactions. *Phycologia* **40**(6), 503–529.
- Pagani M., Freeman K. H., Ohkouchi N., and Caldeira K. (2002) Comparison of water column  $[CO_{2aq}]$  with sedimentary alkenone-based estimates: a test of the alkenone- $CO_2$  proxy. *Paleoceanography* **17**, 1069. doi:10.1029/2002PA000756.
- Pagani M., Zachos J. C., Freeman K. H., Tipler B., and Bohaty S. (2005) Marked decline in atmospheric carbon dioxide concentrations during the Paleogene. *Science* **309**, 600–603.
- Pond D. W., and Harris R. P. (1996) The lipid composition of the coccolithophore *Emiliana huxleyi* and its possible ecophysiological significance. *J. Mar. Biol. Assoc. U.K.* **76**, 579–594.
- Popp B. D., Kenig F., Wakeham S. G., Laws E. A., and Bidigare R. R. (1998a) Does growth rate affect ketone unsaturation and intracellular carbon isotopic variability in *Emiliana huxleyi*? *Paleoceanography* **13**, 35–41.
- Popp B. N., Laws E. A., Bidigare R. R., Dore J. E., Hanson K. L., and Wakeham S. G. (1998b) Effect of phytoplankton cell geometry on carbon isotopic fractionation. *Geochim. Cosmochim. Acta* **62**, 69–77.
- Popp B. D., Prahl F. G., Wallsgrove R. J., and Tanimoto J. (2006) Seasonal patterns of alkenone production in the subtropical oligotrophic North Pacific. *Paleoceanography* **21**(1), PA1004. doi:10.1029/2005PA001165.
- Prahl F. G., and Wakeham S. G. (1987) Calibration of unsaturation patterns in long-chain ketone compositions for paleotemperature assessment. *Nature* **330**, 367–369.
- Prahl F. G., Muehlhausen L. A., and Zahnle D. L. (1988) Further evaluation of long-chain alkenones as indicators of paleoceanographic conditions. *Geochim. Cosmochim. Acta* **52**, 2303–2310.
- Prahl F. G., Herbert T. D., Brassell S. C., Ohkouchi N., Pagani M., Repeta D., Rosell-Melé A., and Sikes E., 2000. Status of alkenone paleothermometer calibration: report from Working Group 3. *Geochem., Geophys., Geosyst.* **1**, Paper number 2000GC000058.
- Prahl F. G., Wolfe G. V., and Sparrow M. A. (2003) Physiological impacts on alkenone paleothermometry. *Paleoceanography* **18**, 1025. doi:10.1029/2002PA000803.
- Prahl F. G., Popp B. N., Karl D. M., and Sparrow M. A. (2005) Ecology and biogeochemistry of alkenone production at Station ALOHA. *Deep Sea Research Part I: Oceanographic Research Papers* **52**(5), 699–719.
- Purdie D. A., and Finch M. S. (1994) Impact of coccolithophorids on dissolved carbon dioxide in sea water enclosures in a Norwegian Fjord. *Sarsia* **79**, 379–387.
- Rau G. H., Riebesell U., and Wolf-Gladrow D. (1996) A model of photosynthetic  $^{13}C$  fractionation by marine phytoplankton based on diffusive molecular  $CO_2$  uptake. *Mar. Ecol. Prog. Ser.* **133**, 275–285.
- Raven J. A., and Johnston A. M. (1991) Mechanisms of inorganic-carbon acquisition in marine phytoplankton and their implications for the use of other resources. *Limnol. Oceanog.* **38**, 1701–1714.
- Riebesell U., Revill A. T., Holdsworth D. G., and Volkman J. K. (2000) The effects of varying  $CO_2$  concentration on lipid composition and carbon isotope fractionation in *Emiliana huxleyi*. *Geochim. Cosmochim. Acta* **64**, 4179–4192.
- Riegman R., Stolte W., Noordeloos A. A. M., and Slezak D. (2000) Nutrient uptake and alkaline phosphatase (EC 3:1:3:1) activity of *Emiliana huxleyi* (Prymnesiophyceae) during growth under N and P limitation in continuous cultures. *J. Phycol.* **36**, 87–96.
- Robertson J. E., Robinson C., Turner D. R., Holligan P., Watson A. J., Boyd P., Fernández E., and Finch M. (1994) The impact of a coccolithophore bloom on oceanic carbon uptake in the northeast Atlantic during summer 1991. *Deep-Sea Res. I* **41**, 297–314.
- Rochelle-Newall E., Delille B., Frankignoulle M., Gattuso J.-P., Jacquet S., Riebesell U., Terbrüggen A., and Zondervan I. (2004) Chromophoric dissolved organic matter in experimental mesocosms maintained under different  $pCO_2$  levels. *Mar. Ecol. Prog. Ser.* **272**, 25–31.
- Rost B., Zondervan I., and Riebesell U. (2002) Light-dependent carbon isotope fractionation in the coccolithophorid *Emiliana huxleyi*. *Limnol. Oceanog.* **47**, 120–128.
- Rost B., Riebesell U., Burkhardt S., and Sültemeyer D. (2003) Carbon acquisition of bloom-forming marine phytoplankton. *Limnol. Oceanog.* **48**, 55–67.
- Rost B., and Riebesell U. (2004) Coccolithophores and the biological pump: responses to environmental changes. In *Coccolithophores—From Molecular Process To Global Impact*, (eds. H.R. Thierstein and J.R. Young), pp. 99–125. Springer.
- Rost B., Riebesell U., and Sültemeyer D. (2006) Carbon acquisition of marine phytoplankton: Effect of photoperiod length. *Limnol. Oceanog.* **51**(1), 12–20.
- Rostek F., Ruhland G., Bassinot F. C., Müller P. J., Labeyrie L. D., Lancelot Y., and Bard E. (1993) Reconstructing sea surface temperature and salinity using  $\delta^{18}O$  and alkenone records. *Nature* **364**, 319–321.
- Sachs J. P., and Lehman S. J. (1999) Subtropical North Atlantic temperatures 60,000 to 30,000 years ago. *Science* **286**, 756–759.
- Sawada K., and Shiraiwa Y. (2004) Alkenone and alkenoic acid compositions of the membrane fractions of *Emiliana huxleyi*. *Phytochemistry* **65**(9), 1299–1307.
- Schantz M. M., Nichols J. J., and Wise S. A. (1997) Evaluation of pressurized fluid extraction for the extraction of environmental matrix reference materials. *Anal. Chem.* **69**, 4210–4219.
- Schouten S., Klein Breteler W. C. M., Blokker P., Schogt N., Rijpstra W. I. C., Grice K., Baas M., and Sinninghe Damsté J. (1998) Biosynthetic effects on the stable carbon isotopic compositions of algal lipids: Implications for deciphering the carbon isotopic biomarker record. *Geochim. Cosmochim. Acta* **62**, 1397–1406.
- Schulte S., Benthien A., Müller P. J., and Rühlemann C. (2004) Carbon isotopic fractionation ( $\epsilon_p$ ) of  $C_{37}$  alkenones in deep-sea sediments: its potential as paleonutrient proxy. *Paleoceanography* **19**, PA1011. doi:10.1029/2002PA000811.
- Sharkey T. D., and Berry J. A. (1985) Carbon isotope fractionation of algae as influenced by an inducible  $CO_2$  concentrating mechanism. In *Inorganic Carbon Uptake By Aquatic Photosynthetic Organisms*, (eds. W.J. Lucas and J.A. Berry), pp. 389–401. The American Society of Plant Physiologists.

- Shifrin N. S., and Chisholm S. W. (1981) Phytoplankton lipids: interspecific differences and effects of nitrate, silicate and light-dark cycles. *J. Phycol.* **17**, 374–384.
- Trimborn S., Langer G., and Rost B., submitted for publication. Effect of varying calcium concentrations and light intensities on calcification and photosynthesis in *Emiliana huxleyi*. *Limnol. Oceanog.*
- Tyrrell T., and Mercio A. (2004) *Emiliana huxleyi*: bloom observations and the conditions that induce them. In *Coccolithophores—From Molecular Processes To Global Impact*, (eds. H.R. Thierstein and J.R. Young), pp. 75–97. Springer.
- Van Bleijswijk J. D. L., Kempers R. S., and Veldhuis M. J. W. (1994) Cell and growth characteristics of types A and B of *Emiliana huxleyi* (Prymnesiophyceae) as determined by flow cytometry and chemical analyses. *J. Phycol.* **30**, 230–241.
- Van Dongen B. E., Schouten S., and Sinninghe Damsté J. S. (2002) Carbon isotope variability in monosaccharides and lipids of aquatic algae and terrestrial plants. *Mar. Ecol. Prog. Ser.* **232**, 83–92.
- Van Emburg P. R., De Jong E. W., and Daems W. T. (1986) Immunochemical localization of a polysaccharide from biomineral structures (coccoliths) of *Emiliana huxleyi*. *J. Ultrastruct. Mol. Struct. Res.* **94**, 246–259.
- Volkman J. K., Barrett S. M., Blackburn S. I., and Sikes E. L. (1995) Alkenones in *Gephyrocapsa oceanica*: implications for studies of paleoclimate. *Geochim. Cosmochim. Acta* **59**, 513–520.
- Westbroek P., Brown C. W., Bleijswijk J. v., Brownlee C., Brummer G. J., Conte M., Egge J., Fernández E., Jordan R., Knappertsbusch M., Stefels J., Veldhuis M., Van der Wal P., and Young J. (1993) A model system approach to biological climate forcing. The example of *Emiliana huxleyi*. *Glob. Planet. Change* **8**, 27–46.
- Williams P. J. I. B., and Egge J. K. (1998) The management and behaviour of the mesocosms. *Est. Coast. Shelf Sci.* **46**, 3–14.
- Winter A., Jordan R. W., and Roth P. H. (1994) Biogeography of living coccolithophores in ocean waters. In *Coccolithophores*, (eds. A. Winter and W.G. Siesser), pp. 161–177. Cambridge University Press.
- Wong W., Sackett W. M., and Benedict C. R. (1975) Isotope fractionation in photosynthetic bacteria during carbon dioxide assimilation. *Plant Physiol.* **55**, 475–479.
- Zondervan I., Rost B., and Riebesell U. (2002) Effect of CO<sub>2</sub> concentration on the PIC/POC ratio in the coccolithophore *Emiliana huxleyi* grown under light-limiting conditions and different daylengths. *J. Exp. Mar. Biol. Ecol.* **272**, 55–70.
- Zondervan I., in press. Factors controlling the ratio of biogenic calcium carbonate to organic carbon production in coccolithophores. *Deep-Sea Res. II*.

Associate editor: H. Rodger Harvey